

Effect of the liquid crystal layer thickness on the optical characteristics of an ultrasound liquid crystal lens

液晶層厚みが超音波式液晶レンズの光学特性に与える影響

Takahiro Iwase[†], Jessica Onaka, Daisuke Koyama, Mami Matsukawa
(Doshisha Univ.)

岩瀬 貴大[†], ジェシカ オナカ, 小山 大介, 松川 真美 (同志社大学)

1. Introduction

Liquid crystal (LC) is intermediate state between the liquid and the solid and has both of liquidity and anisotropy. LCs have various structural phases, and nematic LCs are widely used in optical devices such as LC displays because of high liquidity and optical anisotropy. The molecular orientation of nematic LC can be controlled easily by electric fields using indium tin oxide (ITO) electrodes^[1]. While ITO has high transparency and low electric consumption, ITO contains rare metal indium and the large amounts of equipment are required for the sputtering deposition process^[2]. Our group reported a technique to control the molecular orientation of LC using ultrasound vibration with no ITO electrodes^[3], and an ultrasound variable focus LC lens was developed^[4]. In this paper, the relationship between the thickness of a LC layer and the optical characteristics of an ultrasound LC lens was investigated.

2. Configuration and methods

Fig. 1(A) shows the configuration of the ultrasound variable focus LC lens. Two prototypes were fabricated; a LC layer with a thickness of 100 μm (or 200 μm) was sandwiched by two glass discs (diameters: 15 and 30 mm; thickness: 0.5 mm) using a PET film spacer (we term lens 1 and lens 2, respectively). Orientational films were formed on the surface of the two glass discs for the vertical alignment of the LC molecules. An annular ultrasound PZT transducer (outer diameter: 30 mm; inner diameter: 20 mm; thickness: 1 mm) was attached to the glass disc with a diameter of 30 mm.

By applying a continuous sinusoidal electric signal to the transducer at the resonance frequency of the LC lens, the flexural vibration mode was generated on the lens. The difference of the acoustic energy densities between the LC layer, the glass, and the surrounding medium (air) induces the acoustic radiation force to the lens, resulting in static change in the LC molecular orientation.

Fig. 2 shows the observation system using the LC lens and an optical microscope. The optical characteristics of the lens were evaluated under the

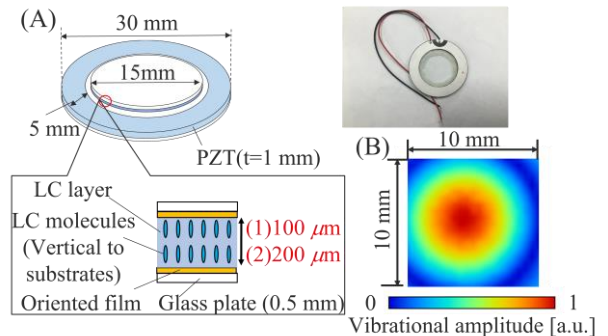


Fig. 1(A) Configuration and (B) vibrational distribution of an ultrasound LC lens.

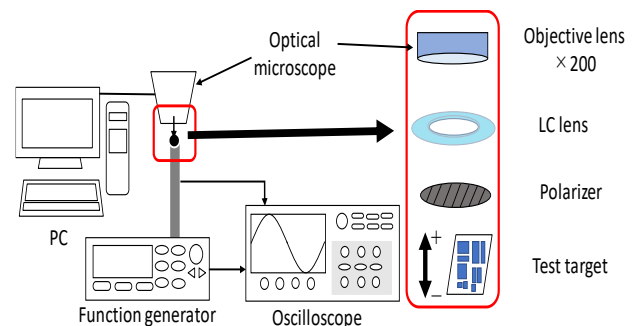


Fig. 2 Observational system using a microscope.

single-Nicol condition using a polarizer. The LC lens was arranged on the optical axis between an objective lens of the microscope and the polarizer, and a test target (1951USAF) was observed through the LC lens. The captured images were analyzed using the image processing software ImageJ to determine the focal point of the LC lens.

3. Results and discussions

The resonance flexural vibration modes were generated at 23 kHz on both two LC lenses. Fig. 1(B) shows the vibrational distribution of the lens 1 at 23 kHz, and the measurement area of 10×10 mm² around the center of the lens was scanned by a laser Doppler vibrometer. The concentric flexural vibration with one nodal circle was generated, and the maximum vibrational displacement amplitude was 9.02 μm when the input voltage was 37 V_{pp}.

Fig. 3 shows the representative microscopic photographs through lens 1 without (Fig. 3(a)) and with ultrasound excitation (Fig. 3(b)). The blurred image (Fig. 3 (a)) changed to the focused image (Fig. 3 (b)), indicating that the focal point was changed along the optical axis by exciting the LC lens ultrasonically.

The focusing characteristics of the LC lenses were evaluated. First, we determined the default position of the test target where the spatial gradient of the image brightness was maximized by moving the test target along the optical axis in the case without ultrasound excitation. Changes in the focal length of the LC lenses were measured by applying the input voltage and moving the test target from the default position. Fig. 4 shows the microscopic images through lens 1 and 2 ((a) and (b) are in the cases for lens 1 excited with 37 V_{pp} and (c) and (d) are for lens 2 with 13 V_{pp}, respectively). By applying the input voltage to the LC lens, the optical images of the target were blurred at the default position (Figs. 4(a) and (c)), and the focused images could be obtained by moving the target 138 μm and 821 μm from the default position in the case of lens 1 and 2, respectively (Figs. 4(b) and (d)). These results mean that changes in the focal lengths of lens 1 and 2 were 138 μm and 821 μm in the case with 37 V_{pp} and 13 V_{pp}, respectively, and the LC lenses acted as a convex lens. Considering the relationship among the voltage amplitude, the change of the focal length, and the thickness of a LC layer, a larger focus shift could be obtained with a thicker LC layer.

The optical characteristics were evaluated by the spatial gradient of the brightness in x and y directions in these images and summarized in Table 1 (the measurement lines are illustrated in Fig. 4(a)). Higher spatial gradient means better image quality; the focused images with sharp edges were captured in Figs. 4(b) and (d).

4. Conclusion

By applying the LC orientation technique using ultrasound vibration, we fabricated two LC lens having a different LC layer thickness (100 and 200 μm) and investigated the relationship between the LC layer thickness and the optical characteristics. Larger focus shift could be realized with thicker LC layer; the maximum focus shift on the LC lens with a 200-μm-thick LC layer was 821 μm.

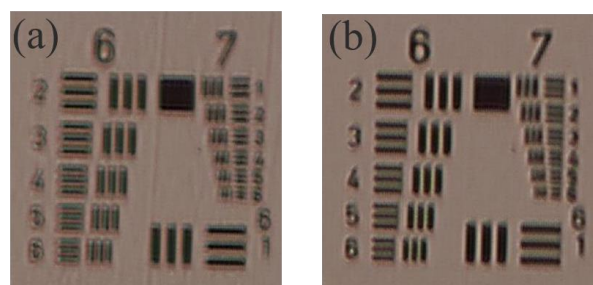


Fig. 3 Representative microscopic images through the LC lens (lens 1) (a) without and (b) with ultrasound vibration at 23 kHz.

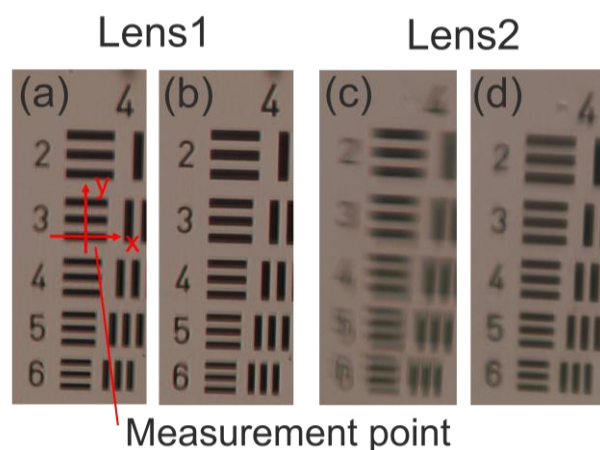


Fig. 4 Microscopic images through two LC lenses ((a) Blurred and (b) focused images for lens 1 with 37 V_{pp} and (c) blurred and (d) focused images for lens 2 with 12.5 V_{pp} at 23 kHz.)

Table 1 Spatial gradients of the brightness in the image captured through lens 1 and 2.

| Lens type direction | Lens1 | | Lens2 | |
|------------------------|-------|-----|-------|-----|
| | (a) | (b) | (c) | (d) |
| X | 5.2 | 11 | 0.94 | 10 |
| Y | 4.6 | 6.9 | 5.9 | 12 |

Unit : Level/ Pixel

Acknowledgment

This work was partly supported by a KAKENHI Grant-in-Aid (No. 19H02056).

References

- [1] M.F. Schiekol and K. Fahrenshon : *Appl. Phys. Lett.*, 19 (1971) 391.
- [2] K. Azuma et al. , *Master. Lett.* , 115, 187 (2014).
- [3] S. Taniguchi, D. Koyama, Y. Shimizu et al. *Appl. Phys. Lett.*108 (2016) 101103.
- [4] Y. Shimizu, D. Koyama, M. Fukui et al. *Appl. Phys. Lett.*112 (2018) 161104.